

## Supporting Information

### Chemical Activity of Oxygen Vacancies on Ceria: A combined Experimental and Theoretical Study on CeO<sub>2</sub> (111)

Chengwu Yang,<sup>a</sup> Li-Li Yin,<sup>b</sup> Fabian Bebensee,<sup>a</sup> Maria Buchholz,<sup>a</sup> Hikmet Sezen,<sup>a</sup> Stefan Heissler,<sup>a</sup> Jun Chen<sup>a</sup>, Alexei Nefedov,<sup>a</sup> Hicham Idriss,<sup>c</sup> Xue-Qing Gong,<sup>\*b</sup> and Christof Wöll<sup>\*a</sup>

<sup>a</sup>Institut für Funktionelle Grenzflächen, Karlsruher Institut für Technologie, 76021 Karlsruhe, Germany

<sup>b</sup>Key Laboratory for Advanced Materials, Centre for Computational Chemistry and Research Institute of Industrial Catalysis, East China University of Science and Technology, Shanghai 200237, P.R. China

<sup>c</sup>Saudi Basic Industries Corporation (SABIC), CRI at KAUST, Thuwal, P.O. Box 4545-4700, Saudi Arabia

#### Content

1. Computational details
2. CO stretch frequency assignments on powder CeO<sub>2</sub>
3. Experimental IRRA spectra of CO on the oxidized CeO<sub>2</sub>(111) surface along the  $[\bar{2}11]$  azimuthal direction
4. Experimental IRRA spectra of CO on the reduced CeO<sub>2</sub>(111) surface along the  $[\bar{2}11]$  azimuthal direction
5. Determination of oxygen vacancy concentration on the oxidized and reduced CeO<sub>2</sub>(111) surfaces from XPS
6. Determination of activation energies ( $E_d$ ) for CO desorption from perfect and defective adsorption sites

## 1. Computational details

The CeO<sub>2</sub>(111) surface was modeled as a periodic slab with three O-Ce-O trilayers of oxide, and the vacuum between slabs was 12 Å. A 4×4 surface cell and corresponding 1×1×1 *k*-point mesh were used in the calculations. Accordingly, the occurrence of a single oxygen vacancy in each surface cell corresponds to oxygen vacancy density of 1/16, or ~6 %, which is rather close to the experimental value of 9%. To represent the electronic structure of Ce 4*f*-orbital adequately, DFT+U with U=5 eV was applied.<sup>1,2</sup> For structure optimization, the ionic positions were allowed to relax until the forces were smaller than 0.05 eV Å<sup>-1</sup> (the bottom trilayer was kept fixed during slab calculations). For the frequency calculations, the movements of the CO molecule, the Ce cations at the adsorption site and all adjacent O<sup>2-</sup> ions were considered. Vibrational frequencies were obtained numerically with four different displacements for each coordinate (NFREE=4). The van der Waals (vdW) interactions were taken into account in all calculations.<sup>3</sup>

## 2. CO stretch frequency assignments on powder CeO<sub>2</sub>

**Table S1.** Frequencies and assignments of CO bands on ceria powders.

$\nu$ (cm <sup>-1</sup> )	Assignments	References
2140	physisorbed CO	[4]
2150 and 2155	CO hydrogen-bonded to OH groups of different acid strengths	
2172	CO interaction with Ce <sup>4+</sup> sites, but actually "more open surface sites"	
2148	physisorbed CO	[5]
2163	CO adsorbed on Ce <sup>3+</sup> sites	
2148 (broad)	CO weakly interacting with the Ce <sup>4+</sup> surface ions	[6]
2151 and 2170	CO on Ce <sup>4+</sup> cations with different coordinative unsaturation	
2157	CO adsorbed on Ce <sup>3+</sup> sites	
2140	liquid-like CO	
2145 (shoulder)	liquid-like CO phase	[7]
2159	non-specific interactions	
2169	Lewis centers	
2140	liquid-like CO (tridimensional phase)	[8]
2151-2157	physisorbed CO weakly interacting with the surface (bi-dimensional phase)	
2162-2168	CO coordinated to Ce <sup>4+</sup> cations	
2143	physisorbed CO at 80 K	[9]
2149	perturbed adsorbed species	
2153-2157	CO bound to Ce <sup>4+</sup> (V <sub>O</sub> ), i.e., to Ce <sup>4+</sup> in the vicinity of an oxygen vacancy	
2169-2176	CO bound to Ce <sup>4+</sup>	
2148.5-2145.5	very weak interaction of CO with the surface	[10]
2161	Ce <sup>3+</sup> (CO) surface species	
2169	Ce <sup>4+</sup> (CO) surface species	
2150	CO adsorbed on Ce <sup>3+</sup>	[11]
2170	CO adsorbed on coordinatively unsaturated Ce <sup>4+</sup>	
2170-2150	CO linearly adsorbed on coordinatively unsaturated Ce <sup>4+</sup> ions	[12]
2127-2120	CO-Ce <sup>3+</sup> species and electronic transition	
2156	CO linearly adsorbed on Ce <sup>4+</sup> in a more unsaturated coordination state	[13]
2177	CO linearly adsorbed on Ce <sup>4+</sup>	
2162	CO on Ce <sup>3+</sup>	[14]

3. Experimental IRRA spectra of CO on the oxidized  $\text{CeO}_2(111)$  surface along the  $[-211]$  azimuthal direction

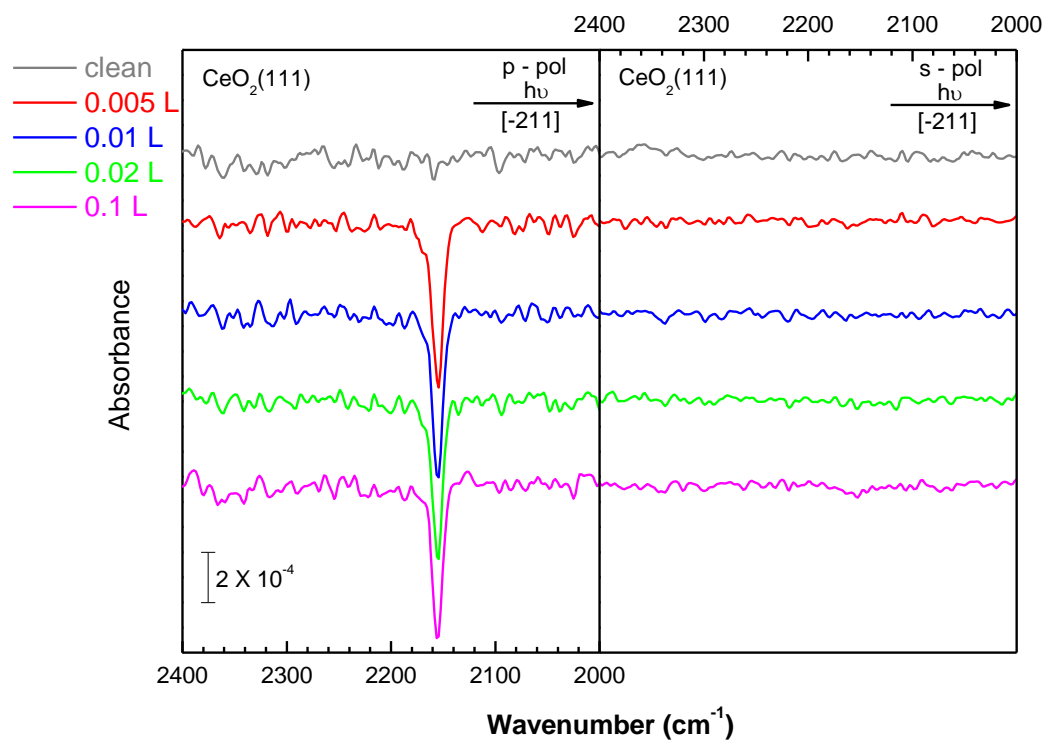


**Fig. S1.** Experimental IRRA spectra of different doses of CO at 71 K on the fully oxidized  $\text{CeO}_2(111)$  at a grazing incidence angle of  $80^\circ$  with (left)  $p$ - and (right)  $s$ -polarized light incident along  $[-211]$ .

4. Experimental IRRA spectra of CO on the reduced  $\text{CeO}_2(111)$  surface along the  $[-211]$  azimuthal direction

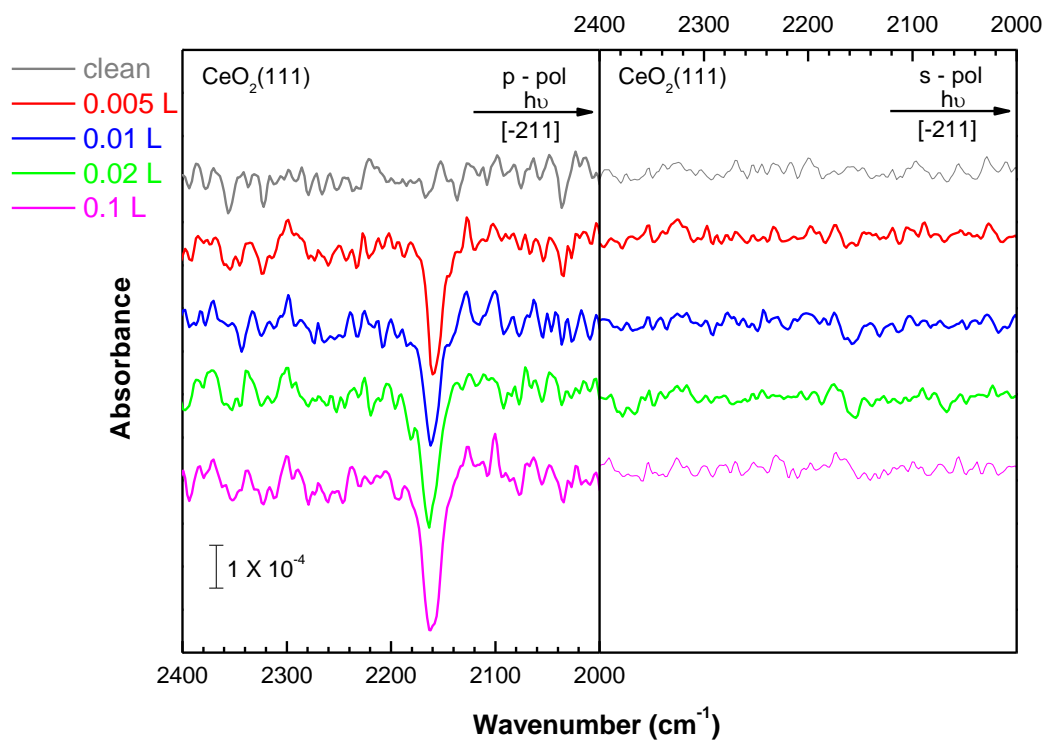


**Fig. S2.** Experimental IRRA spectra of different doses of CO at 68 K on the reduced  $\text{CeO}_2(111)$  at a grazing incidence angle of  $80^\circ$  with (left)  $p$ - and (right)  $s$ -polarized light incident along  $[-211]$ .

5. Determination of oxygen vacancy concentration on the oxidized CeO<sub>2</sub>(111) surface from XPS

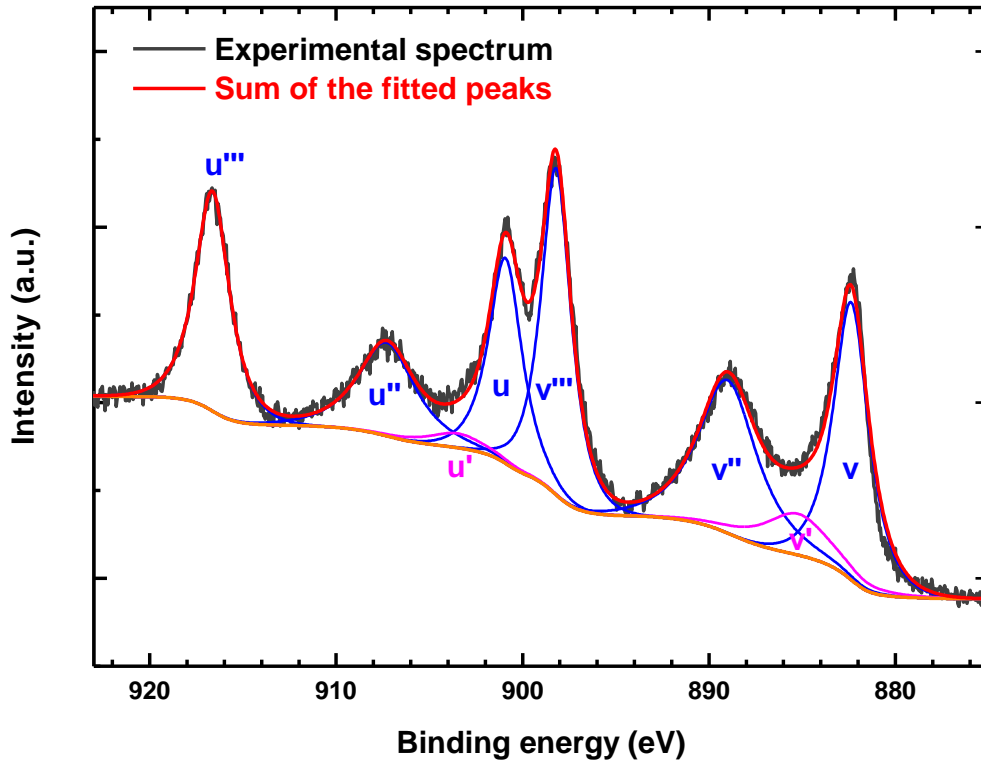


**Fig. S3.** Fitted Ce 3d XP spectrum of the oxidized CeO<sub>2</sub>(111).

Ce 3d XP spectrum was fitted with ten peaks and the labels follow the convention established by Burroughs et al.,<sup>15</sup> in which u and v refer to the 3d<sub>3/2</sub> and 3d<sub>5/2</sub> spin-orbit components, respectively. The u''', u'', u and v''', v'', v peaks are attributed to Ce<sup>4+</sup> final states, while the u', u<sub>0</sub> and v', v<sub>0</sub> are attributed to Ce<sup>3+</sup> final states.<sup>16</sup> We fixed the peak positions based on Preisler et al.'s assignments.<sup>17</sup> Note that the contribution of the v<sub>0</sub> and u<sub>0</sub> peaks for Ce<sup>3+</sup> can be disregarded in the spectrum with low Ce<sup>3+</sup> ion concentrations.<sup>18</sup>

The concentration of Ce<sup>3+</sup> within the CeO<sub>2</sub>(111) surface can be determined from the following equations:<sup>19</sup>

$$\text{Ce(III)} = v' + v_0 + u' + u_0 \quad (1)$$

$$\text{Ce(IV)} = u''' + u'' + u + v''' + v'' + v \quad (2)$$

$$\text{Ce(III)} = \frac{\text{Ce(III)}}{\text{Ce(III)} + \text{Ce(IV)}} \quad (3)$$

**Table S2.** Components for Ce3d spectrum of the oxidized CeO<sub>2</sub>(111).

<b>Ce3d<sub>5/2</sub></b>	<b>u'''</b>	<b>u''</b>	<b>u'</b>	<b>u</b>
Origin	Ce <sup>4+</sup>	Ce <sup>4+</sup>	Ce <sup>3+</sup>	Ce <sup>4+</sup>
Position	916.64	u''' - 9.35	u''' - 13.15	u''' - 15.72
FWHM	2.16	3.60	3.60	2.10
Area	1322805.0	937372.5	140336.0	1202520.0
<b>Ce3d<sub>3/2</sub></b>	<b>v'''</b>	<b>v''</b>	<b>v'</b>	<b>v</b>
Origin	Ce <sup>4+</sup>	Ce <sup>4+</sup>	Ce <sup>3+</sup>	Ce <sup>4+</sup>
Position	u''' - 18.44	u''' - 27.64	u''' - 31.4	u''' - 34.27
FWHM	1.90	3.60	4.15	2.2
Area	1730318.0	1558449.7	477052.1	1726106.5

The fit of the spectrum of the oxidized surface (Fig. S3) is in very good agreement with the measured spectrum. According to the above equation, the Ce<sup>3+</sup> concentration was determined to be 6.7%. Due to two Ce<sup>3+</sup> cations corresponding to one oxygen vacancy (O<sub>v</sub>) and Ce/O atomic ratio in CeO<sub>2</sub> of 1/2, the density of oxygen vacancies (O<sub>v</sub>) on the oxidized CeO<sub>2</sub>(111) surface therefore amounts to 1.7%.

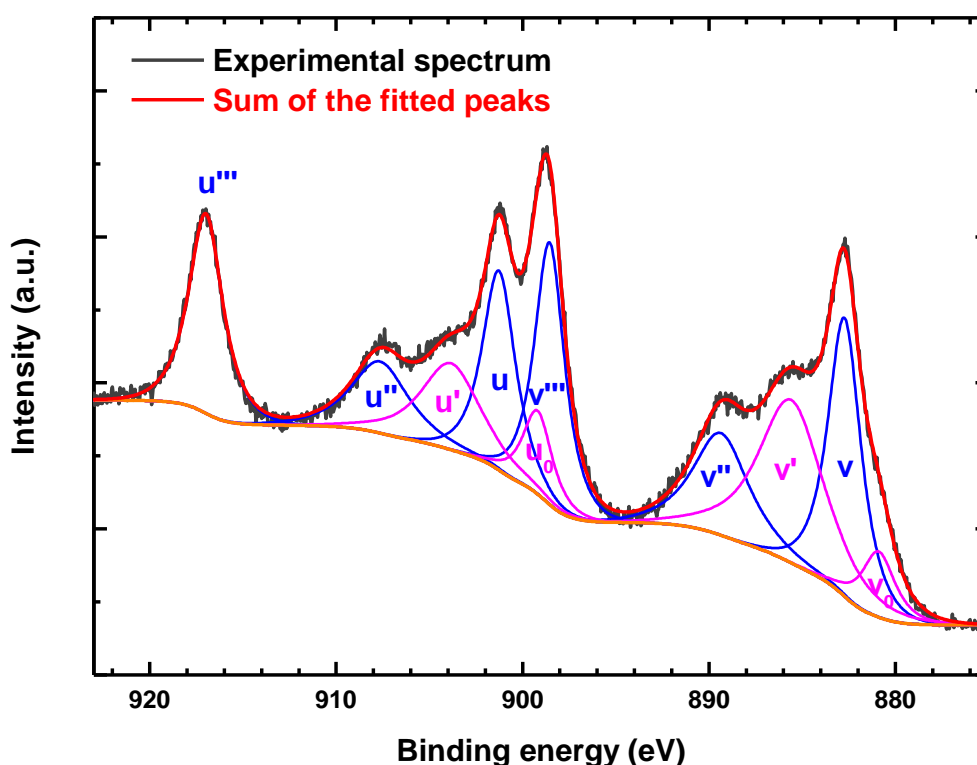


**Fig. S4.** Fitted Ce3d XP spectrum of the reduced CeO<sub>2</sub>(111).

To get a consistent fit result for the Ce3d XP spectrum of the reduced CeO<sub>2</sub>(111), we used the same fitting parameters (line shape, peak positions, and full width at half maximums (FWHMs)) as in the fit of the Ce3d XP spectrum of the oxidized CeO<sub>2</sub>(111). The concentration of Ce<sup>3+</sup> on the reduced CeO<sub>2</sub>(111) surface is 33% determined by

the calculation method described above using the intensities of the various peaks given in Table S3. The corresponding density of oxygen vacancies ( $O_v$ ) on the reduced  $CeO_2(111)$  surface is approximately 9%.

**Table S3.** Components for  $Ce3d$  spectrum of the reduced  $CeO_2(111)$ .

<b>Ce3d<sub>5/2</sub></b>	<b>u'''</b>	<b>u''</b>	<b>u'</b>	<b>u</b>	<b>u<sub>0</sub></b>
Origin	Ce <sup>4+</sup>	Ce <sup>4+</sup>	Ce <sup>3+</sup>	Ce <sup>4+</sup>	Ce <sup>3+</sup>
Position	916.99	u''' - 9.35	u''' - 13.15	u''' - 15.72	u''' - 17.8
FWHM	2.16	3.60	3.60	2.10	1.84
Area	1444225.9	889274.1	1052711.0	1424875.5	523896.5
<b>Ce3d<sub>3/2</sub></b>	<b>v'''</b>	<b>v''</b>	<b>v'</b>	<b>v</b>	<b>v<sub>0</sub></b>
Origin	Ce <sup>4+</sup>	Ce <sup>4+</sup>	Ce <sup>3+</sup>	Ce <sup>4+</sup>	Ce <sup>3+</sup>
Position	u''' - 18.44	u''' - 27.64	u''' - 31.4	u''' - 34.27	u''' - 36.1
FWHM	1.90	3.60	4.15	2.20	2.06
Area	1667934.2	1238930.4	2185115.8	2071862.1	403663.9

6. Determination of activation energies ( $E_d$ ) for CO desorption from perfect and defective adsorption sites

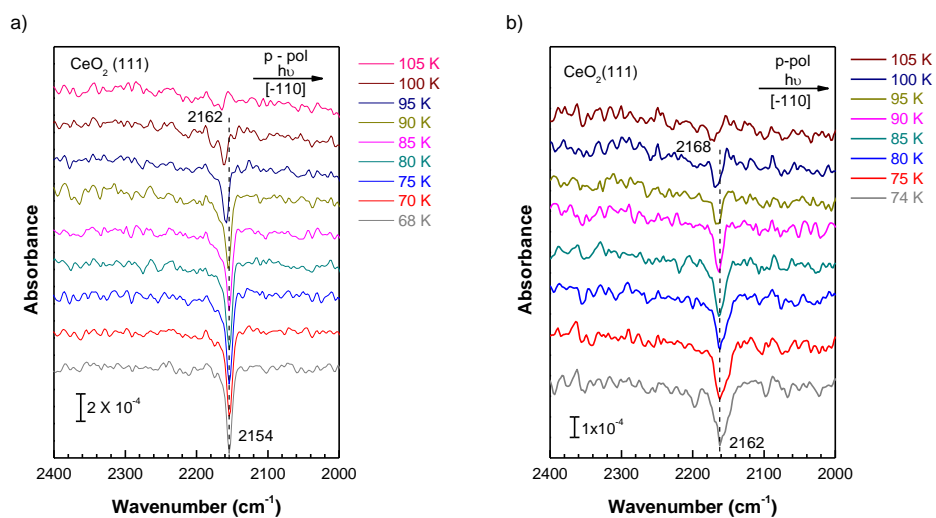


**Fig. S5.** Experimental IRRA spectra recorded directly after dosing of 0.1 L CO at ceria surfaces (lowest traces). The samples were gradually heated and spectra were recorded at the temperatures indicated. (a) CO on fully oxidized ceria surface, (b) CO on reduced surface.

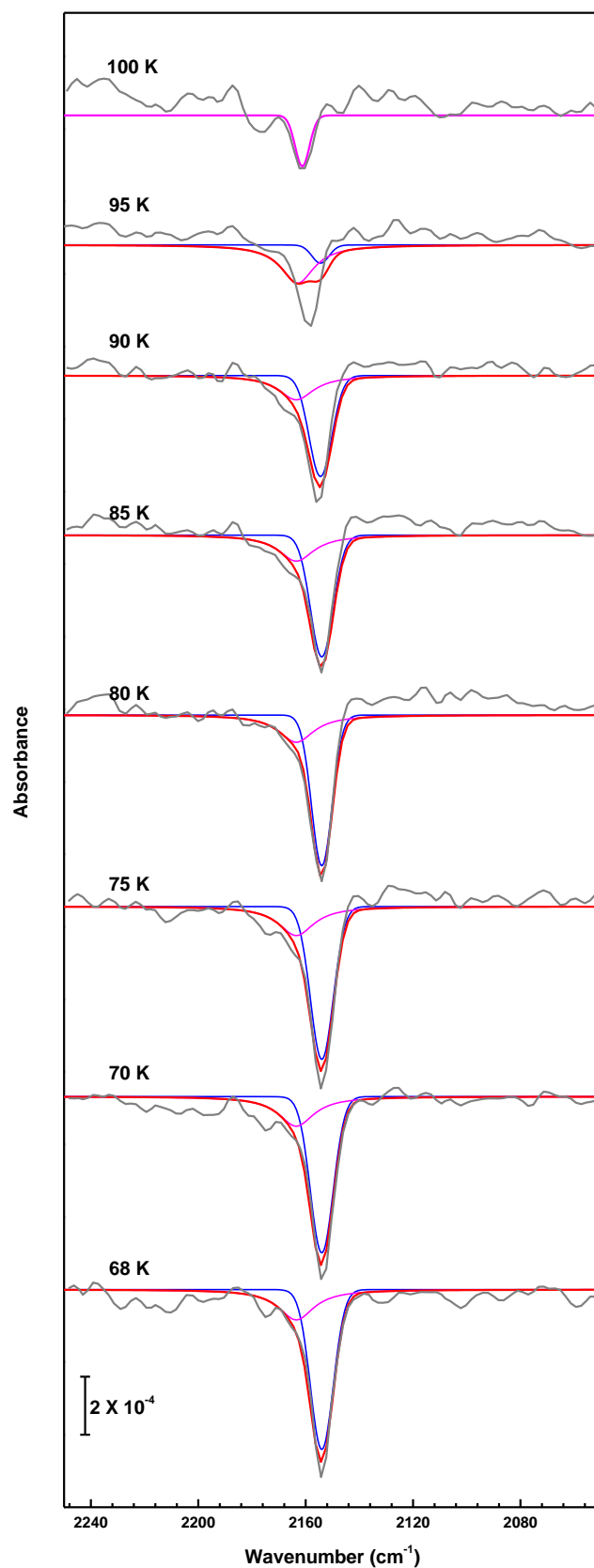


**Fig. S6.** IR bands and fitted peaks of CO during desorption from the oxidized surface.

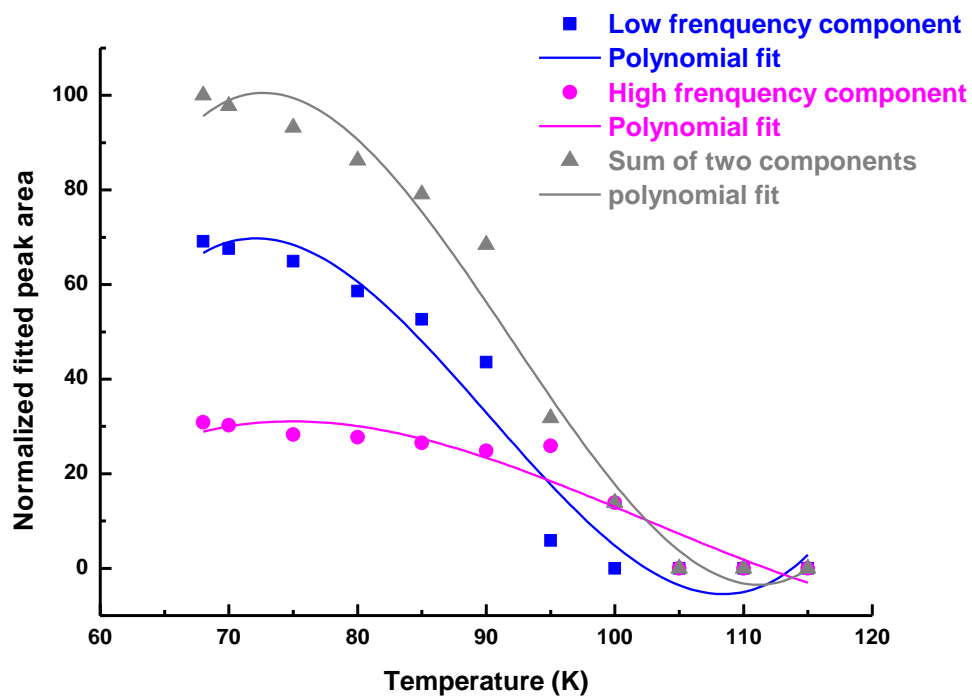


**Fig. S7.** Fit curves for normalized fitted peak areas of components in IR bands of CO during desorption from the oxidized surface.

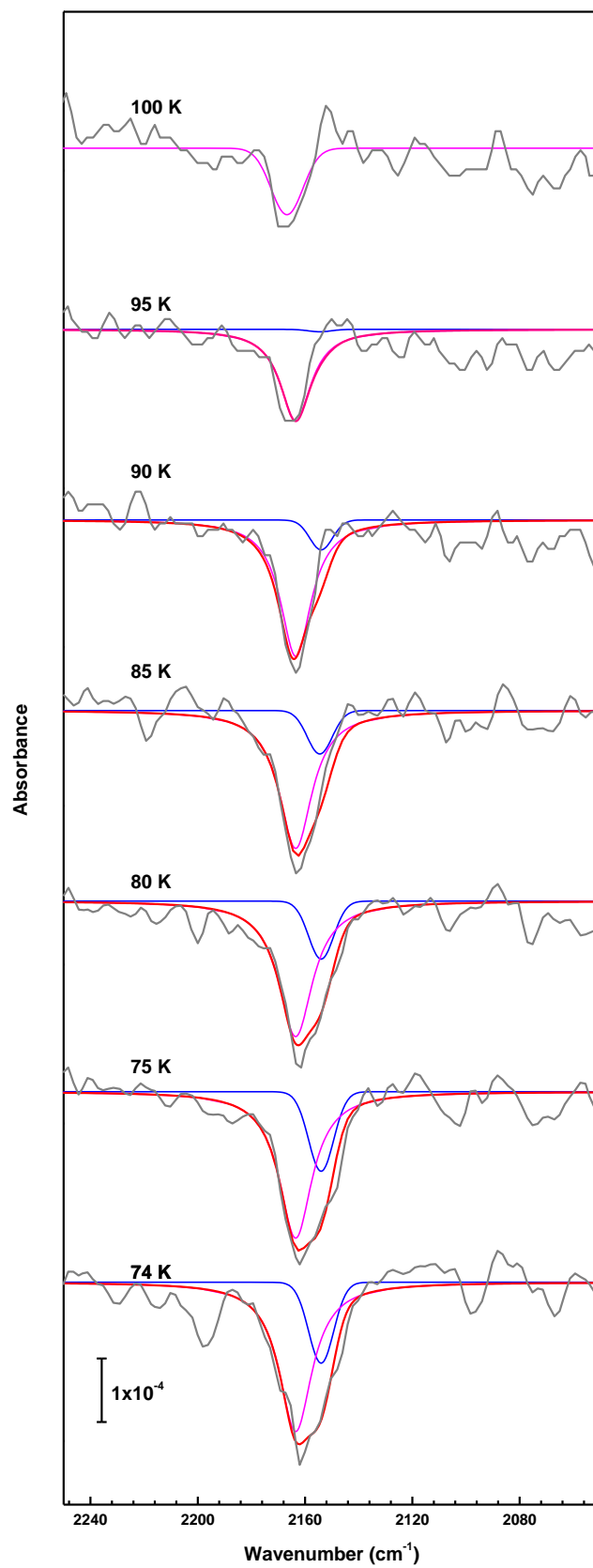


**Fig. S8.** IR bands and fitted peaks of CO during desorption from the reduced surface.

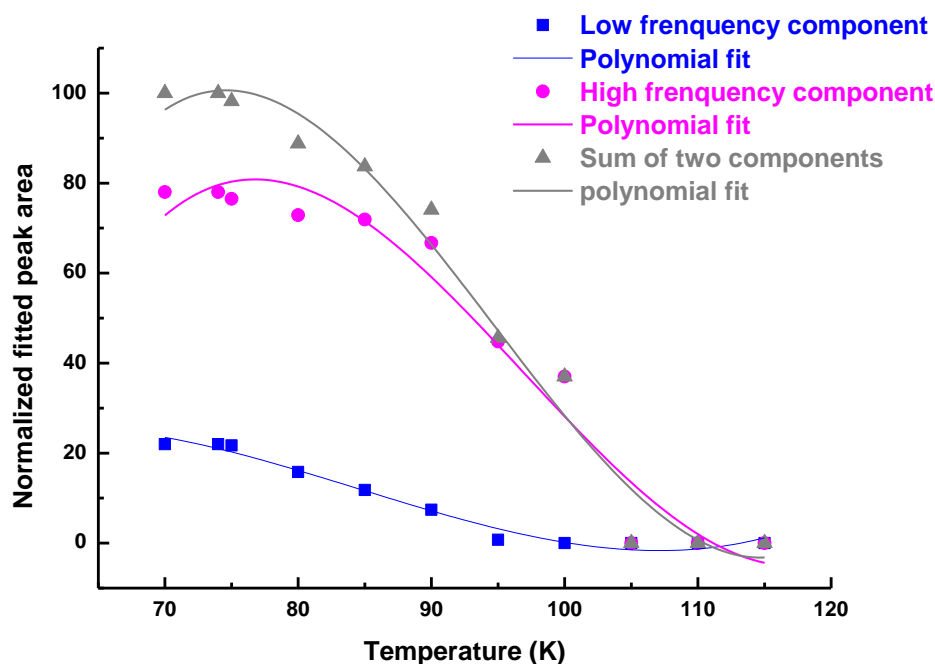


**Fig. S9.** Fit curves for normalized fitted peak areas of components in IR bands of CO during desorption from the reduced surface.

Since the IR band of CO on the oxidized surface (bottommost spectrum in Fig. S5a) is sharp and symmetric with only a minute shoulder at high frequency, we first fitted this band to determine the peak position and FWHM of the predominant low frequency component. We obtained a frequency of  $2154\text{ cm}^{-1}$  and a FWHM of  $10\text{ cm}^{-1}$  for this feature.

We also considered the IR spectra recorded for CO adsorbed on the reduced surface (bottommost spectrum in Fig. S5b) with a much broader band. Assuming only a single additional component to the one described above, we find the new band centered at  $2163\text{ cm}^{-1}$  with a FWHM of  $16\text{ cm}^{-1}$ .

Keeping these fitting parameters constant, we subsequently conducted peak fittings on all of the IR spectra shown in Fig. S5. The corresponding results are displayed in Fig. S6 and Fig. S8. Note that the fitting has a less quality at higher temperature due to the lower intensity and more deviated from the temperature where the background acquired. Generally, it is qualitatively visible from both sets of spectra that high frequency component is more stable and diminishes at higher temperatures, which was confirmed by the curve fitting and calculated  $E_d$  values.

We extracted the peak areas as a function of temperature from the peak fits (see Figs. S6 and S8) and determined the temperatures of the desorption rate maximum ( $T_{max}$ ) from derivatives of the peak areas for the stoichiometric and the reduced surface. We find values of approximately 88 K and 100 K for CO desorption from perfect sites and defective sites, respectively.

Employing the Redhead equation<sup>20</sup> to estimate the activation energies ( $E_d$ ) for CO desorption from these two different adsorption sites yields values of 0.27 eV for perfect sites and 0.31 eV for defective sites.

$$E_{d1} \approx RT_{\max} \left[ \ln \left( \frac{v_{1T_{\max}}}{\beta_H} \right) - 3.64 \right] = 8.314 \times 10^{-3} \times 88 \times [\ln(10^{13} \times 88 / 0.01) - 3.64]$$

$$= 25.9 \text{ kJ/mol} = 0.27 \text{ eV}$$

$$E_{d2} \approx 8.314 \times 10^{-3} \times 100 \times [\ln(10^{13} \times 100 / 0.01) - 3.64] = 29.5 \text{ kJ/mol} = 0.31 \text{ eV}$$

## References

- (1) Nolan, M.; Grigoleit, S.; Sayle, D. C.; Parker, S. C.; Watson, G. W. *Surface Science* **2005**, 576, 217.
- (2) Nolan, M.; Parker, S. C.; Watson, G. W. *Surface Science* **2005**, 595, 223.
- (3) Grimme, S. *Journal of computational chemistry* **2006**, 27, 1787.
- (4) Farra, R.; Wrabetz, S.; Schuster, M. E.; Stotz, E.; Hamilton, N. G.; Amrute, A. P.; Perez-Ramirez, J.; Lopez, N.; Teschner, D. *Physical chemistry chemical physics : PCCP* **2013**, 15, 3454.
- (5) Bazin, P.; Saur, O.; Lavalley, J. C.; Daturi, M.; Blanchard, G. *Physical Chemistry Chemical Physics* **2005**, 7, 187.
- (6) Tabakova, T.; Boccuzzi, F.; Manzoli, M.; Andreeva, D. *Applied Catalysis A: General* **2003**, 252, 385.
- (7) Daturi, M.; Binet, C.; Lavalley, J.-C.; Galtayries, A.; Sporcken, R. *Physical Chemistry Chemical Physics* **1999**, 1, 5717.
- (8) Binet, C.; Daturi, M.; Lavalley, J.-C. *Catalysis Today* **1999**, 50, 207.
- (9) Mekhemer, G. A. H.; Zaki, M. I. *Adsorption Science & Technology* **1997**, 15, 377.
- (10) Badri, A.; Binet, C.; Lavalley, J.-C. *Journal of the Chemical Society, Faraday Transactions* **1996**, 92, 1603.
- (11) Zaki, M. I.; Vielhaber, B.; Knoezinger, H. *The Journal of Physical Chemistry* **1986**, 90, 3176.
- (12) Bozon-Verduraz, F.; Bensalem, A. *Journal of the Chemical Society, Faraday Transactions* **1994**, 90, 653.
- (13) Li, C.; Sakata, Y.; Arai, T.; Domen, K.; Maruya, K.-i.; Onishi, T. *Journal of the Chemical Society, Faraday Transactions 1: Physical Chemistry in Condensed Phases* **1989**, 85, 929.
- (14) Mudiyansele, K.; Kim, H. Y.; Senanayake, S. D.; Baber, A. E.; Liu, P.; Stacchiola, D. *Physical chemistry chemical physics : PCCP* **2013**, 15, 15856.
- (15) Burroughs, P.; Hamnett, A.; Orchard, A. F.; Thornton, G. *Journal of the Chemical Society, Dalton Transactions* **1976**, 1686.
- (16) Kotani, A.; Jo, T.; Parlebas, J. C. *Advances in Physics* **1988**, 37, 37.
- (17) Preisler, E. J.; Marsh, O. J.; Beach, R. A.; McGill, T. C. *Journal of Vacuum Science & Technology B: Microelectronics and Nanometer Structures* **2001**, 19, 1611.
- (18) Celardo, I.; De Nicola, M.; Mandoli, C.; Pedersen, J. Z.; Traversa, E.; Ghibelli, L. *ACS Nano* **2011**, 5, 4537.
- (19) Pfau, A.; Schierbaum, K. D. *Surface Science* **1994**, 321, 71.
- (20) Redhead, P. A. *Vacuum* **1962**, 12, 203.